Van der Waals Interactions Between Organic Adsorbates and at Organic/Inorganic Interfaces

Alexandre Tkatchenko, Lorenz Romaner, Oliver T. Hofmann, Egbert Zojer, Claudia Ambrosch-Draxl, and Matthias Scheffler

Abstract

Van der Waals (vdW) interactions play a prominent role in the structure and function of organic/organic and organic/inorganic interfaces. Their accurate determination from first principles, however, is a notoriously difficult task. Recently, a surge of interest in modeling vdW interactions has led to promising theoretical developments. This article reviews the state-of-the-art of describing vdW interactions by density-functional theory with respect to accuracy and practicability. The performance of the different methods is demonstrated for simple systems, such as rare-gas dimers and small organic molecules. The nature of binding at organic/inorganic interfaces is then exemplified for the perylene-3,4,9,10-tetracarboxylic-3,4,9,10-dianhydride (PTCDA) molecule at surfaces of coinage metals. This fundamental system is the best-characterized organic molecule/metal interface in experiment and theory. We emphasize the crucial importance of a balanced description of both geometry and electronic structure in order to understand and model the properties of such systems. Finally, the relevance of vdW interactions to the function of actual devices based on interfaces is discussed.

Introduction

Bonding at organic/organic and organic/inorganic interfaces results from interplay of several interactions, most notably (covalent) hybridization of wave functions, electron transfer processes, van der Waals (vdW) interaction, and Pauli repulsion. Typically, one distinguishes different bonding regimes: In the case of pure physisorption, the attraction between the adsorbate and the substrate is mainly due to vdW forces, which are, hence, essential for a correct description. Standard systems characterized by vdW bonding are molecules adsorbed on the basal plane of graphite.[1,2] An intermediate bonding regime arises for π-conjugated molecules adsorbed on metal surfaces where also electron transfer processes and covalent bonding come into play.[3–9] In this context, we will discuss the adsorption of perylene-3,4,9,10-tetracarboxylic-3,4,9,10-dianhydride (PTCDA) on Ag(111) as an example, as this is one of the best-characterized metal/organic interfaces both in experiment and in theory.[36] For this and similar systems, vdW forces are found to be crucial for obtaining reliable geometries and energies. Interestingly, vdW interactions play a noticeable role even for chemisorption when strong chemical bonds are formed between docking groups of a molecule and the substrate (e.g., for self-assembled monolayers [SAMs] bonded to gold by thiolates).[10] Here they can decisively influence the molecular tilting angle, molecular distortions, or isomerization.[3] Not surprisingly, the interface geometry is crucial for its electronic properties, which, in turn, control the function of organic devices. In particular, the interface dipole, and hence the alignment of the molecular electronic states with respect to the Fermi level of the electrode, are sensitive to the atomic positions.

Generally, the term "vdW forces" can refer to different types of intermolecular interactions, such as electrostatics (permanent multipole–permanent multipole interaction), induction (permanent multipole–induced multipole interaction), and dispersion (induced multipole–induced multipole interaction). Dispersion usually is the strongest attractive term for molecules physisorbed or weakly chemisorbed on surfaces. Hence, the term "dispersion energy" is frequently used interchangeably with "vdW energy," and we follow this convention in this article. The dispersion energy arises from the correlated motion of electrons and must be described by many-electron quantum mechanics. Unfortunately, accurate quantum-chemical calculations are only feasible in the near future for finite systems up to ~100 light atoms. Thus, for most systems of interest in interface modeling, fully first-principles calculations of vdW forces are not realistic at present. However, for many situations, alternative approaches exist that have comparable accuracy, and we will discuss these approaches in the next section, particularly concentrating on Kohn-Sham density-functional theory (DFT). Our main focus is on methods that currently show the most promise, contain few empirical parameters, and have already been applied to the modeling of interfaces. Next, the influence of vdW interactions for the geometry and electronic structure of an organic/inorganic model system—PTCDA on Ag(111)—will be discussed. Lastly, it will be shown that vdW interactions also play a prominent role in determining the structure and function of real interfaces, such as SAMs on metal surfaces.

Methods for Treating van der Waals Interactions

Noncovalent vdW forces are crucial for the formation, stability, and function of molecules and materials. The vdW dispersion energy arises from the correlated motion of

electrons and must be described by many-electron quantum mechanics. Based on electronic structure, there are two primary approaches for calculating vdW interactions: the quantum-chemical wave function methods based on Hartree-Fock (HF) and methods rooted in Kohn-Sham DFT. Both HF and Kohn-Sham DFT are based on an independent-electron picture. HF theory is self-interaction free (the electrostatic interaction of an electron with itself is exactly canceled), and it provides a natural starting point for including electron correlation (quantum many-body effects) with computationally expensive wave function–based methods. On the other hand, DFT, together with standard exchange-correlation (xc) functionals (local density approximation [LDA], Perdew-Burke-Ernzerhof [PBE]), contains spurious self-interaction but provides a route to include electron correlation effects in an effective way at a relatively low computational cost. However, the electron correlation in DFT is usually of (semi-)local origin (i.e., an electron only "sees" other electrons in its close vicinity). See Tables I and II for brief descriptions of DFT-based

Table I. Brief Descriptions, Advantages, and Shortcomings of DFT-Based Electronic Structure Methods.

Method	Description	Advantages	Shortcomings
DFT	Density-functional theory. The ground-state properties of an interacting many-electron system are uniquely determined by its electron density $n[\mathbf{r}]$. Nobel prize to W. Kohn for the development of DFT in 1998.	In principle, DFT is exact. Typically, it is employed in the Kohn-Sham form with an approximate electron exchange-correlation (xc) functional. Existing approximations to the xc functional yield good accuracy for many applications.	Improvement toward "better" functionals is not systematic.
LDA	Local-density approximation to the exchange-correlation functional in DFT. The xc energy at each spatial point only depends on the electron density at that point.	Exact for the homogeneous electron gas. Lattice constants of solids predicted within 2% of experiment (underestimated). Applicable to big systems (thousands of atoms).	Overestimates solid cohesive energies and bulk moduli by 10%–20%. Large overestimation of intermolecular interaction energies (30%). No vdW interactions. Self-interaction error (an electron interacts with itself) results in an adequate description of electronic spectra and electron transfer.
GGA (e.g., PBE[54] or revPBE[25])	Generalized-gradient approximation to the xc functional in DFT. The xc energy also depends on the density gradient at a point. The construction of GGAs is not unique. PBE: Perdew-Burke-Ernzerhof functional. revPBE: revised PBE functional of Zhang and Yang. Fits exact exchange energy of rare-gas atoms.	Partially corrects the LDA for inhomogeneous electron densities. Molecular atomization energies are significantly improved. Lattice constants of solids within 2% of experiment using PBE (overestimated). Applicable to big systems (thousands of atoms).	Underestimates solid cohesive energies and bulk moduli by 10%–20%. Large underestimation of intermolecular interaction energies (60%). No vdW interactions. Self-interaction error still present.
DFT-D[22]	Corrects DFT by adding interatomic vdW C_6R^{-6} interaction, with empirical C_6 coefficients and cutoff at short distances.	Remarkable accuracy for intermolecular interactions (15%–20% error for energies and 0.1–0.2 Å for equilibrium distances). Can be connected to different DFT xc functionals. Same computational cost as the underlying DFT calculation.	Needs at least two empirical parameters for each atom in the periodic table. Does not describe different possible hybridization states of an atom in a molecule. Empirical connection between DFT and the vdW energy tail. Not yet applied to solids.
DFT+vdW[24]	Corrects DFT by adding interatomic vdW $C_6[n]R^{-6}$ interactions, with $C_6[n]$ coefficients and vdW radii obtained from the DFT electron density (n).	Remarkable accuracy for intermolecular interactions (8% error for energies and 0.1 Å for equilibrium distances). Handles different hybridization states transparently. Can be connected to different DFT xc functionals. Same computational cost as the underlying DFT calculation.	Empirical connection between DFT and the vdW energy tail. Not yet applied to solids.

Continued

Table I. Brief Descriptions, Advantages, and Shortcomings of DFT-Based Electronic Structure Methods. (*Continued*)

Method	Description	Advantages	Shortcomings
vdW-DF[20]	Van der Waals density functional by Langreth and Lundqvist. Non-local xc functional to treat vdW interactions in DFT. It employs the revPBE functional for exchange and the LDA for local correlation.	First-principles solution without empiricism. Has been applied to molecules and solids. Computational cost comparable with DFT-PBE.	Errors of 20%–30% for intermolecular energies and 0.3–0.4 Å for equilibrium distances. Accuracy for solids not yet fully established.
cRPA[15]	Correlation energy employing the random-phase approximation. Presently the most sophisticated approximation to the correlation energy in DFT.	"Seamless" treatment of vdW interactions at all distances for molecules and solids. Remarkable performance for lattice constants (1.4%) and bulk moduli of solids (11%).[53]	Computationally expensive (applicable to systems <100 atoms). So far done non-self-consistently, thus results are sometimes sensitive to input orbitals (DFT-LDA, DFT-PBE, etc.).
GW	*G*: Green's function. *W*: Screened Coulomb interaction. Many-body approach for the calculation of the photoemission spectrum.	Quasi-particle (electron and hole) energies in agreement with experimental photoelectron spectroscopies.	Calculations of total energies still rare. So far done non-self-consistently, thus results are sometimes sensitive to input orbitals (DFT-LDA, DFT-PBE, etc.).
ACFD[16]	Adiabatic-connection fluctuation-dissipation theorem. Connects the independent-electron Kohn-Sham system with the full quantum many-body electronic system.	Allows obtaining *exact* xc functional in DFT. Equivalent to the full solution of the quantum many-body problem.	Calculations not feasible for any real system.

Table II. Brief Description, Advantages, and Shortcomings of Wave Function–Based Electronic Structure Methods.

Method	Description	Advantages	Shortcomings
Wave function–based electronic structure methods	Methods that directly employ the electronic wave function with $3N$ coordinates, where N is the number of electrons.	Well-defined hierarchy of approximations toward *exact* treatment of exchange and correlation.	Accurate methods are very expensive in computational time and memory requirements.
HF	Hartree-Fock. Self-consistent exact-exchange method. The "base" for all quantum chemical approaches.	Free from self-interaction error.	No correlation energy included. Considerably underestimates the binding in molecules and solids. Highly problematic for metals. No vdW interactions.
MP2	Møller-Plesset second-order perturbation theory. Wave function–based method to include correlation energy on top of HF.	Accurate molecular geometries. Can be applied to systems of up to ~500 atoms. VdW interactions approximately included.	VdW interactions overestimated by 30%–50%.
MP2+ΔvdW[14]	MP2 with the $C_6[n]R^{-6}$ vdW energy correction.	Same computational cost as MP2. Similar accuracy for intermolecular interactions as with very expensive CCSD(T).	Requires cutoff function at short distances.
CCSD(T)	Coupled cluster method with single, double, and perturbative triple electron excitations. Considered "gold standard" in quantum chemistry.	Remarkable accuracy for intermolecular binding energies and geometries. Seamless inclusion of all electron correlation effects, including vdW interactions.[11]	Computationally very expensive (applicable to systems of 20–50 light atoms). Not directly applicable to solid-state systems.

and wave function–based theoretical methods used in this work, along with their advantages and shortcomings.

The HF method does not describe the dispersion interaction by definition, since dispersion arises solely from electron correlation. Thus, higher level approaches built on top of HF need to be employed, such as Møller-Plesset second-order perturbation theory (MP2), or the coupled cluster method.[11] Unfortunately, coupled cluster theory with single, double, and perturbative triple excitations (CCSD(T))—the quantum-chemical "gold standard"—becomes unfeasible for systems larger than about 50 light atoms (and even for the simplest periodic systems) due to its steep increase in computational cost with system size. More affordable MP2 calculations (applicable up to ~200–500 light atoms with state-of-the-art implementations) unfortunately overestimate the dispersion energy by nearly a factor of two for π-π stacked systems,[12] though corrections for this problem have been recently proposed.[13,14]

DFT calculations are used routinely to study the structure and electronic properties of interfaces, being applicable to systems comprising tens of thousands of electrons. In principle, DFT is exact. However, in practice, the xc energy functional has to be approximated, and also state-of-the-art (semi-)local or hybrid xc functionals do not properly account for the dispersion interaction. An exact route toward the description of vdW interactions in DFT is provided by the adiabatic-connection fluctuation-dissipation (ACFD) theorem,[15,16] which connects the independent-electron Kohn-Sham system with a fully interacting electronic many-body system. Full ACFD-DFT calculations, however, are unfeasible, hence approximations must be employed. The most promising route is combining the exact treatment of exchange with the random-phase approximation for electron correlation (EX+cRPA), which has recently gained popularity.[9,15,17,18] However, even EX+cRPA is computationally intensive and so far can only be applied to rather small systems (clusters and periodic systems with less than about 100 light atoms). Furthermore, EX+cRPA is still an approximation to the exact treatment of exchange and correlation, and it is sometimes sensitive to the input orbitals (LDA, PBE).

Motivated by the need to address larger and more complex systems, numerous other, more feasible, approaches have been proposed for including vdW interactions in DFT. Among the most promising ones, one may distinguish the Langreth-Lundqvist density functional (vdW-DF)[19–21] on the one hand (described in the next paragraph) and corrections based on a summation of dispersion energy contributions between all atoms in the system (DFT-D and DFT+vdW)[22–24] on the other. Both routes describe the long-range vdW interaction and, at atomic overlap regions, link it to a "standard" exchange-correlation functional.

Langreth et al. developed the vdW-DF functional over the last decade.[19–21] Like the RPA, it is based on the ACFD theorem. Characteristic for DFT calculations, the corresponding nonlocal correlation energy contribution is obtained from the electron density only. The local electron correlation is treated by LDA, while the exchange energy is described by the generalized gradient approximation (GGA) to the xc functional, specifically the so-called revPBE[25] functional. The approach is very attractive, as it is derived from first principles and does not rely on empirical parameters or fitting. With recent implementations,[26,27] its computational efficiency is comparable to that of standard DFT-GGA calculations. However, especially for intermolecular interactions, the performance of vdW-DF is not spectacular, as can be seen in Figures 1 and 2. The improvement of vdW-DF is an active research field, and recent developments yield better accuracy by employing different exchange functionals than revPBE for the short range and/or by introducing parameters fitted to high-level quantum-chemical binding energies.[28,29]

The alternative DFT-D approach simply adds the interatomic dispersion energy contributions to DFT total energies, typically only considering the leading-order $C_6 R_{ij}^{-6}$ term, where R_{ij} is the distance between atoms i and j, and C_6 is the associated dispersion coefficient. The DFT-D approach has gained popularity after Grimme showed that accurate results for intermolecular interactions can be achieved, and DFT-D can be connected to different functionals.[22] The main shortcoming of previous DFT-D formulations is the high level of empiricism, requiring at least two fitting parameters for every element in the periodic table. Furthermore, different possible hybridization/oxidation states of atoms in different chemical or geometrical environments were not accounted for. Recently, several groups have proposed different solutions to these issues.[24,30–32] In particular, Tkatchenko and Scheffler developed a method to obtain accurate dispersion coefficients and vdW radii directly from the ground-state molecular or condensed matter electron density (DFT+vdW method).[24] This approach starts from high-level quantum-chemistry calculations for free atoms, and then the *changes* that result from the interactions between atoms are obtained from the electron density of the polyatomic system. There is a single parameter remaining in the DFT+vdW method, the vdW radius scaling. This parameter defines the linkage of the R^{-6} vdW interaction and the DFT functional, as originally proposed by Hobza and co-workers.[23] This linkage is achieved by introducing a so-called damping function that multiplies the R_{ij}^{-6} interaction and smoothly cuts it off at short interatomic distances. This function and its onset parameter, the vdW radius, remain the main weakness of the approach. A strength of the DFT+vdW method and of the general DFT-D concept is that they can be easily coupled to different xc functionals. Later in this section, we restrict the

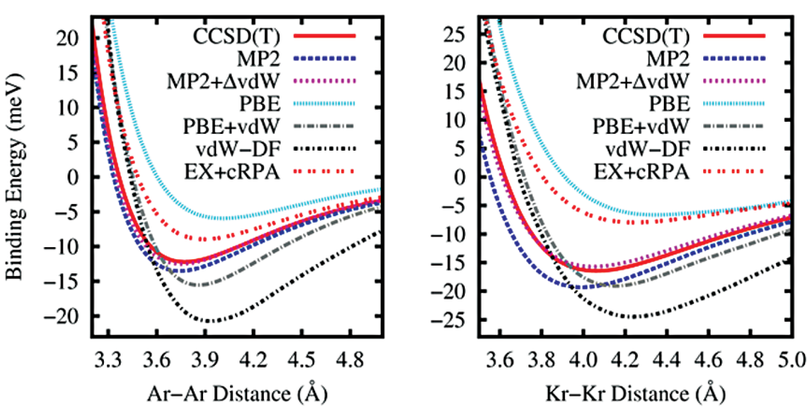

Figure 1. Performance of different approximate electronic structure methods for the description of the binding-energy curves of (a) argon (Ar) and (b) krypton (Kr) dimers. The reference results are given by CCSD(T)—coupled cluster method with single, double, and perturbative triple electron excitations. See Tables I and II for a detailed explanation of different electronic structure methods.[14,20,24]

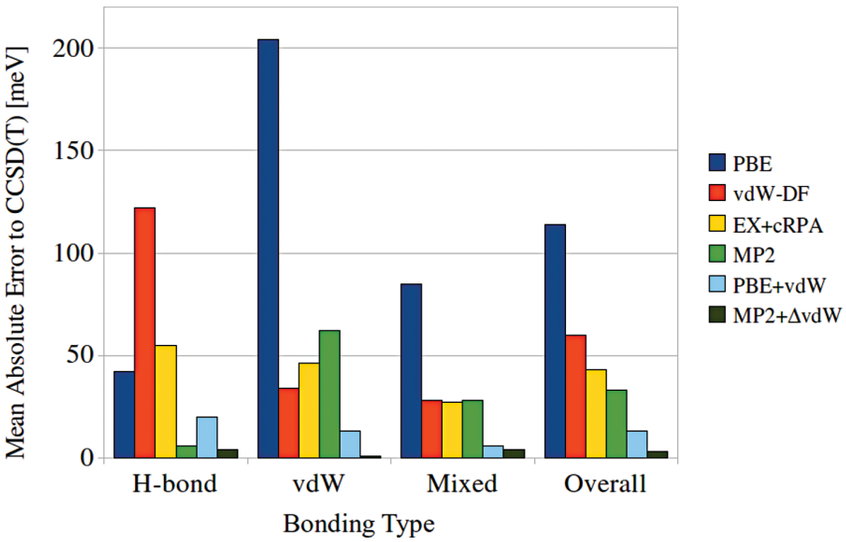

Figure 2. Performance of different approximate electronic structure methods on the binding energies of 22 dimers with noncovalent intermolecular interactions (S22 database).[12] The reference values are given by CCSD(T)—coupled cluster method with single, double, and perturbative triple electron excitations. See Tables I and II for a detailed explanation of different electronic structure methods. The MP2+ΔvdW method has only been applied to a subset of 16 systems, for which atomic projection of dispersion coefficients is possible.[12,14,22,24,27]

discussion to the PBE xc functional, and therefore label the approach as PBE+vdW (PBE-D when using the approach by Grimme[22]). PBE is used since it is a non-empirical xc functional that yields accurate results for both molecules and solids. Let us note that the concept of the semi-empirical correction also has been carried over to quantum-chemical methods, such as MP2, with success.[14]

To illustrate the performance of vdW-DF and PBE+vdW methods, we show in Figure 1 the binding-energy curve for the argon and krypton dimers—fundamental vdW-bonded systems. The reference calculations refer to CCSD(T), and they typically reproduce experimental data within a few percent. All calculations are fully converged, with estimated deviations of less than 1 meV from the complete basis set limit. The vdW-DF overestimates both the equilibrium distance (by 0.2–0.3 Å) and the binding energy (by 40%–60%). There are two main reasons for these deviations: the errors in the calculated C_6 dispersion coefficients (~20%) and the use of the revPBE functional for the local regime. The PBE+vdW method also overbinds, but with somewhat smaller error. The recently developed dispersion-corrected MP2 approach (MP2+ΔvdW)[14] consistently achieves CCSD(T)-quality at significantly smaller computational cost. Similar conclusions hold for the whole S22 database of noncovalent interactions introduced by Hobza et al.,[12] as shown in Figure 2. Most members of the quantum chemistry community consider this database to be arguably the most accurate for intermolecular interactions; it contains converged CCSD(T) results for the binding energies of 22 organic dimers, including vdW, electrostatic, and hydrogen bonding. The standard PBE functional significantly underestimates the binding energies with a mean absolute error (MAE) of 114 meV. In contrast, MP2 overestimates the dispersion interactions, yielding considerable error for vdW-bonded systems with a MAE of 33 meV. The vdW-DF functional underestimates the binding in hydrogen-bonding systems with a MAE of 59 meV on the S22 database. Its performance can be improved by choosing a different DFT exchange functional, however this comes at the expense of significantly larger errors in case of vdW-bonding.[27] The PBE+vdW method further reduces the error on the S22 database to 13 meV, showing similar accuracy for hydrogen and vdW-bonded systems. Finally, MP2+ΔvdW yields an almost negligible MAE of 3 meV from the CCSD(T) reference data.

It is widely assumed that vdW interactions have a minor direct effect on the electronic structure. While the semi-empirical DFT-D methods do not affect the electronic structure by construction, a self-consistent vdW-DF approach, in principle, can modify the electronic structure. However, the changes due to vdW interactions were found to be very small for selected test cases.[33] In contrast, it is well known that the influence of vdW interactions on the geometry of molecules can be significant. Obviously, such geometry changes will, in turn, have a profound influence on the electronic structure. In some cases, GGA density functionals, when using the correct (experimental) geometry, are sufficient to yield electronic properties in qualitative agreement with experiment, but, in many cases, hybrid functionals, which include a fraction of HF exchange, are needed for an appropriate description. Recently, this issue has been illustrated for the example of metal-phthalocyanine dimers.[34] While both methods, PBE+vdW and PBE-hybrid+vdW, yielded essentially the same geometry, only the hybrid functional could reproduce experimental photoemission spectra. We remark in passing that accurate many-body approaches (such as *GW*, where *G* is Green's function and *W* is the screened Coulomb interaction) can be used as well for calculating the electronic spectrum,[35] and this is, in fact, the more general and systematic route. However, the discussion of such approaches is beyond the scope of the present article.

Organic/Inorganic Interfaces

After reviewing the methodology, we will now address the role of vdW forces for bonding at organic/inorganic interfaces with the π-conjugated molecule PTCDA adsorbed on Ag(111) as an example. The chemical structure of PTCDA is shown at the bottom right of Figure 3. This is one of the best characterized metal/organic interfaces, both experimentally and theoretically.[36] Regarding the geometric and electronic structure of the interface, the following key parameters are known from experimental investigations of the highly ordered room-temperature phase:

1. The molecular monolayer adsorbs at a distance of 2.86 Å from the surface with the carboxylic oxygen atoms, which are located at the corner of the molecule, 0.18 Å below the carbon backbone, indicative of a covalent attraction.[37] These results were obtained from x-ray standing wave measurements which, for well-ordered systems, allow a determination of atomic positions within a few hundredths of an Å.
2. The formerly lowest unoccupied molecular level (LUMO) of the PTCDA molecule is located right at the Fermi level (E_F) in the adsorbate system.[38] Its partial occupation reflects a metal to molecule electron transfer.
3. At the same time, the work function of the Ag(111) surface increases by 0.1 eV at

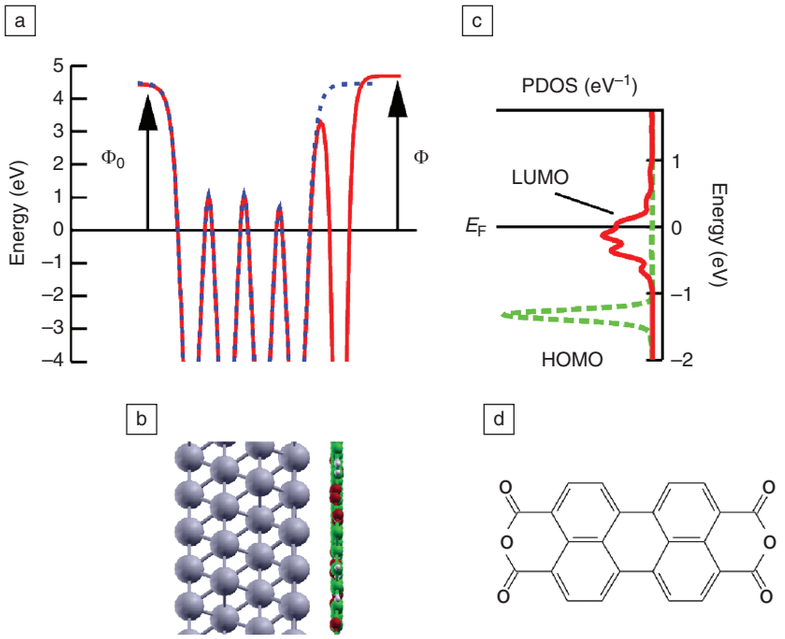

Figure 3. (a) Plane-averaged electrostatic potential of the substrate without (dotted line) and with (solid line) the adsorbed PTCDA (perylene-3,4,9,10-tetracarboxylic-3,4,9,10-dianhydride) monolayer. The work function of the bare Ag surface is given by Φ_0 and that of the covered surface by Φ. (b) Side view of the metal/organic interface with the slab being modeled with four layers on the left and the monolayer adsorbed onto the right surface. (c) Projected density of states (PDOS) onto the LUMO (lowest unoccupied molecular level) and the HOMO (highest occupied molecular orbital) of PTCDA. (d) Illustration of the chemical structure of PTCDA.

monolayer coverage.[38] Considering that weakly interacting non-polar molecules typically lower the work function by 0.5–1.0 eV due to the so-called push-back effect,[39] the increase observed here reflects the electron-accepting properties of PTCDA at this surface. The term "push-back" refers to the fact that Pauli repulsion between the occupied states of the molecule and the substrate leads to a mutual polarization that reduces the surface dipole of the metal substrate and, as a consequence, its work function.[39]

4. The adsorption energy of PTCDA cannot be verified directly in desorption experiments, as this requires that the molecule desorbs as a whole, while PTCDA desorbs in fragments. However, a very similar molecule, which is half the size of PTCDA, has an adsorption energy on Ag(111) of 1.2 eV.[40] Thus, the adsorption energy of PTCDA is expected to be around 2.4 eV.

As a first step, we address the performance of DFT-PBE for describing the electronic structure of the monolayer. The calculations were performed by constraining the carbon atoms to be located at the experimentally determined position while fully optimizing all remaining degrees of freedom.[8] In agreement with experiment, the oxygen atoms are found 0.11 Å below the carbon backbone. The position of the LUMO for the adsorbed molecule is displayed in Figure 3, as inferred from the density of states projected onto the orbitals of the free molecule (projected density of states or PDOS). The corresponding maximum is right below the Fermi level, and, hence, a large fraction of the metal-LUMO hybrid orbitals are occupied in agreement with UPS data. The highest-occupied molecular orbital (HOMO) level is calculated to be 1.2 eV below the LUMO, which also compares well with the experimental value of about 1.5 eV. As (semi-)local exchange-correlation functionals, such as DFT-PBE, underestimate the bandgap of PTCDA and molecules in general (due to self-interaction and the missing discontinuity of the exchange-correlation potential), the good agreement found for the adsorbate case may appear surprising. However, as noted previously, upon adsorption, the formerly empty LUMO became more delocalized and fractionally occupied, which can be expected to partly remove this underestimation. Furthermore, as shown by Neaton and coworkers,[41] (semi-)local exchange-correlation functionals miss a correlation contribution arising from surface polarization. This stabilizes the LUMO and destabilizes the HOMO and, therefore, partly compensates the remaining self-interaction error.

Due to the metal-molecule interaction, the potential felt by electrons at the interface is modified, as indicated in Figure 3. To the left, it is plotted for the bare Ag slab (blue, dotted line) and for the interface (red, full line). The work function Φ_0 of the bare Ag surface is defined as the difference between the Fermi level and the vacuum level at the uncovered surface. The work function Φ of the covered surface is given by the vacuum level to the right of the total system, and we find that it has increased by about 0.2 eV compared to Φ_0, in reasonable agreement with experiment (0.1 eV). As we also had seen that most of the LUMO-derived DOS got filled by electrons, this change of the work function might appear rather small. Indeed, a more extensive analysis[8] shows that the work function increase due to the LUMO filling is counteracted by electron back transfer, Pauli repulsion, and bending of the molecule. Moreover, also some charge (~0.5 electrons) is transferred from the metal to the molecule, which weakens the push-back effect. A similar agreement with experimental observations has been found for PTCDA on Cu(111) and Au(111).[8] On the latter surface, the LUMO remains essentially unoccupied, reflecting that Φ_0 of Au(111) is larger than that of Ag(111), and the work function is reduced.

The PBE functional fails when describing the correct adsorption distance and energy. The energy is repulsive everywhere, as shown in Figure 4 as a function of distance. Hence, PBE underestimates the bonding strength for PCTDA at Ag(111) and fails as severely with respect to energetics and geometry as for purely vdW-bound systems. Again, this finding holds true also for PTCDA adsorbed onto Cu(111) and Au(111)[8] and was observed for these surfaces and also for other molecules such as benzene or azobenzene.[3–5] On more reactive surfaces, such as Cu(110), PBE can give rise to binding (e.g., for a thiophene ring[7] or a benzene ring[6]). However, in all cases, inclusion of vdW forces has been found to strongly modify adsorption energies and distances.

As explained in the previous section, there are several ways to incorporate vdW interactions to improve on PBE calculations. Figure 4a shows results for PTCDA on Ag(111) using the vdW-DF approach. The nonlocal vdW energy, E_{nl}, is negative (i.e., attractive) and decreases monotonically with increasing distance. At the experimental binding distance, the contribution from this quantity amounts to several eVs.

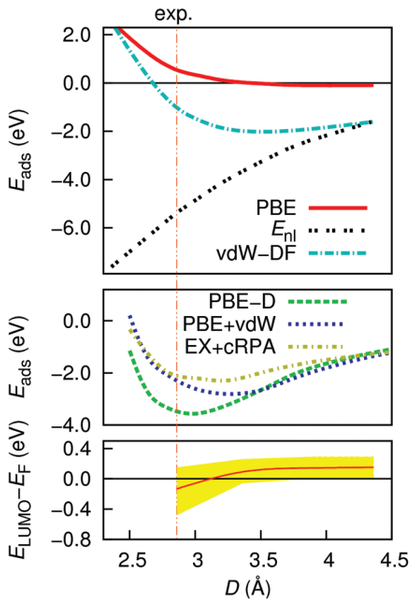

Figure 4. (a) Adsorption energy for PTCDA (perylene-3,4,9,10-tetracarboxylic-3,4,9,10-dianhydride) adsorbed onto Ag(111) when employing PBE and vdW-DF.[6] Also shown is E_{nl}, which is the non-local correlation term in vdW-DF. The experimental value is indicated by the horizontal red line labeled "exp." (b) Adsorption energy obtained with PBE-D,[3] PBE+vdW,[3] and EX+cRPA.[7] (c) Position of the LUMO (lowest unoccupied molecular level) relative to the Fermi level. The red line indicates the peak maximum, while the peak width is evidenced in yellow. Note that the width does not decrease to zero at high adsorption distances, as a minimum width is required in the density-functional theory calculations of metals. D, adsorption distance.

The total interaction energy obtained by vdW-DF displays a pronounced minimum of about 2 eV per molecule at a bonding distance of 3.5 Å. Hence, vdW-DF gives realistic adsorption energies but overestimates adsorption distances as already found in the previous section for intermolecular interactions.

Results obtained by different semi-empirical methods[3–5] and EX+cRPA[9] are shown in Figure 4b. All curves exhibit a sizable minimum in the adsorption energy, but the spread between the methods is considerable, with adsorption energies ranging between 2 to 4 eV and adsorption distances between 3 and 3.5 Å. The two main differences between DFT-D and DFT+vdW are the use of different C_6 coefficients and different damping functions. Both DFT-D and DFT+vdW methods do not yet describe the screening of the vdW interaction by the metal bulk, thus the application to metals represents an approximation. These aspects and the applicability of different DFT-D methods to the modeling of adsorption on metal surfaces were discussed in detail.[3–5] For the vdW-DF method, the influence of approximations, such as the use of revPBE for the exchange part, the approximate treatment for the polarizability (plasmon-pole model), and the neglect of electron-density gradient terms in the correlation energy, still needs to be examined. Lastly, we note that for computational feasibility, some assumptions and approximations were required also when applying the EX+cRPA approach.[9] A common trend for all methods is the overestimation of binding distances. For a correct description of interface phenomena, this geometry uncertainty is problematic, as it can lead to qualitative errors in the electronic structure. For example, as shown in Figure 4c, the peak maximum of the LUMO-related PDOS moves through the Fermi level only at adsorption distances below 3 Å, and the peak position and width around the experimental equilibrium geometry depend sensitively on the adsorbate distance.[8] Extending the vdW-DF to investigations to Au and Cu substrates[8] reveals little influence of the substrate on the bonding distances. This is, however, in contrast to the experimental findings that place the molecule much closer to the substrate in the Cu case than for Au. Hence, while the discussed methods give much more realistic binding energies and distances than PBE, they still need to be improved for a reliable first-principles description of the geometry.

Relevance of vdW Interactions for Organic Devices

Obviously, the careful control of interface properties is crucial for the function of organic devices;[43] for example, they determine injection and extraction barriers in light-emitting diodes, thin-film transistors, and solar cells. Consequently, a variety of procedures has been developed to tune the electronic characteristics of interfaces toward optimum functionality. These techniques include, among others, the usage of SAMs,[44,45] redox-doping,[46] or the deposition of (sub)monolayers of strong electron acceptors or donors.[47,48] To optimize such techniques and to allow for a rational design of new organic molecules, an in-depth understanding of interfaces also at an atomistic level is important.[49,50] So far, this is best obtained by a combined theoretical and experimental approach (see References 51 and 52). For strongly bonded systems, such as 2-(4-dicyanomethylene-2,3,5,6-tetrafluoro-cyclohexa-2,5-dienylidene)-malononitrile (F4TCNQ) on noble metals[51] or covalently bonded SAMs,[52] excellent results for geometry and electronic structure can be obtained in the framework of DFT using (semi-)local exchange-correlation functionals. However, for the vast majority of the practically relevant systems, a proper inclusion of vdW interactions is essential for obtaining reasonable adsorption geometries, as already illustrated in the previous sections. Unfortunately, despite the success of present procedures, their accuracy is still not sufficient to credit them with predictive power.

The structure of covalently bonded SAMs is also affected by vdW interactions similar to single molecule adsorption geometries. For example, it has been found[52] that PBE calculations underestimate the tilt-angle measured by near-edge x-ray adsorption for a well-ordered anthracene selenolate SAM on Au(111), while the overestimation of the intermolecular interactions in LDA results in a tilt that is too large. Preliminary studies employing DFT-D indicate that the inclusion of vdW interactions gives rise to an intermediate situation in better agreement with the experiment.[52] Such issues can become important for SAM-induced work-function changes when using molecules bearing significant long-axis dipole moments.

Moreover, situations exist in which the inclusion of vdW forces affects the relative energetics of different adsorption geometries of an organic/inorganic system. A prototypical example here is azobenzene,[3–5] which can occur in the cis- or the trans-conformation. Standard DFT calculations predict that for adsorption on Ag(111), the cis-conformation is energetically more favorable. The vdW interactions, however, stabilize the trans-conformation to a larger amount than the cis-isomer because of its larger contact area with the surface; the amount of stabilization is high enough here where the trans-isomer becomes the global minimum. As the cis-trans isomerization changes both the molecular dipole moment and the interaction with the substrate, this affects the adsorption-induced work function.

Summary and Outlook

Van der Waals (vdW) interactions are ubiquitous intermolecular forces that play a crucial role in determining the geometry of interfaces, and, consequently, have a large effect on the functionality of organic devices. Recently, several promising methods (DFT+vdW and vdW-DF) have been developed to include vdW interactions in density-functional theory calculations at moderate or no additional computational cost. For the interaction between atoms and small molecules, "chemical accuracy" of 1 kcal/mol can

be achieved with some vdW-corrected methods. Unfortunately, this is not yet the case for organic/inorganic interfaces.

With the example of PTCDA on Ag(111), we have illustrated that the Perdew-Burke-Ernzerhof (PBE) functional can capture the relevant features in the interfacial charge density, and the resulting work-function change is obtained quite reliably. A prerequisite, however, hence the essence of a successful vdW approach, is to properly describe the adsorption geometry. The latter has a profound effect on the push-back, the metal-to-molecule charge transfer, as well as on the magnitude and orientation of intrinsic or adsorption-induced molecular dipole moments. In spite of the promising approaches currently available for treating vdW interactions, the obtained results show a considerable spread. Part of the shortcomings can be related to the underlying approximations and the fact that the treatment of metallic systems is still an open issue. The huge demand for an equally feasible as well as reliable scheme has triggered tremendous activities in this research field in view of which major improvements can be expected in the future.

Acknowledgments

We acknowledge financial support from the Marie Curie Network SMALL, the Austrian Science Fund (FWF), projects P9714 and P20972-N20. A.T. thanks the Alexander von Humboldt (AvH) Foundation. We acknowledge the Kavli Institute of Theoretical Physics at the University of California, Santa Barbara, where part of this paper was written (supported in part by the National Science Foundation under Grant No. PHY05-51164).

References

1. F. Ortmann, W.G. Schmidt, F. Bechstedt, *Phys. Rev. Lett*. **95**, 186101 (2005).
2. S.D. Chakarova-Käck, E. Schröder, B.I. Lundqvist, D.C. Langreth, *Phys. Rev. Lett*. **96**, 146107 (2006).
3. E. McNellis, J. Meyer, K. Reuter, *Phys. Rev. B* **80**, 205414 (2009).
4. G. Mercurio, E. McNellis, I. Martin, S. Hagen, F. Leyssner, S. Soubatch, J. Meyer, M. Wolf, P. Tegeder, F.S. Tautz, K. Reuter, *Phys. Rev. Lett*. **104**, 036102 (2010).
5. E. McNellis, PhD thesis, Fritz-Haber-Institut der MPG (2010).
6. N. Atodiresei, V. Caciuc, P. Lazic, S. Blügel, *Phys. Rev. Lett*. **102**, 136809 (2009).
7. P. Sony, P. Puschnig, D. Nabok, C. Ambrosch-Draxl, *Phys. Rev. Lett*. **99**, 176401 (2007).
8. L. Romaner, D. Nabok, P. Puschnig, E. Zojer, C. Ambrosch-Draxl, *New J. Phys*. **11**, 053010 (2009).
9. M. Rohlfing, T. Bredow, *Phys. Rev. Lett*. **101**, 266106 (2008).
10. G. Heimel, L. Romaner, J.-L. Bredas, E. Zojer, *Phys. Rev. Lett*. **96**, 196806 (2006).
11. C.D. Sherrill, T. Takatani, E.G. Hohenstein, *J. Phys. Chem. A* **113**, 10146 (2009).
12. P. Jurečka, J. Sponer, J. Černý, P. Hobza, *Phys. Chem. Chem. Phys*. **8**, 1985 (2006).
13. A. Hesselmann, *J. Chem. Phys*. **128**, 144112 (2008).
14. A. Tkatchenko, R.A. DiStasio Jr., M. Head-Gordon, M. Scheffler, *J. Chem. Phys*. **131**, 094106 (2009).
15. D. Bohm, D. Pines, *Phys. Rev*. **92**, 609 (1953).
16. D.C. Langreth, J.P. Perdew, *Phys. Rev. B* **15**, 2884 (1977).
17. X. Ren, P. Rinke, M. Scheffler, *Phys. Rev. B* **80**, 045402 (2009).
18. J. Harl, G. Kresse, *Phys. Rev. Lett*. **103**, 056401 (2009).
19. Y. Andersson, D.C. Langreth, B.I. Lundqvist, *Phys. Rev. Lett*. **76**, 102 (1996).
20. M. Dion, H. Rydberg, E. Schröder, D.C. Langreth, B.I. Lundqvist, *Phys. Rev. Lett*. **92**, 246401 (2004).
21. D.C. Langreth, B.I. Lundqvist, S.D. Chakarova-Käck, V.R. Cooper, M. Dion, P. Hyldgaard, A. Kelkkanen, J. Kleis, L. Kong, S. Li, P.G. Moses, E. Murray, A. Puzder, H. Rydberg, E. Schröder, T. Thonhauser, *J. Phys. Condens. Matter* **21**, 084203 (2009).
22. S. Grimme, *J. Comput. Chem*. **27**, 1787 (2006).
23. P. Jurečka, J. Černý, P. Hobza, D.R. Salahub, *J. Comput. Chem*. **28**, 555 (2006).
24. A. Tkatchenko, M. Scheffler, *Phys. Rev. Lett*. **102**, 073005 (2009).
25. Y. Zhang, W. Yang, *Phys. Rev. Lett*. **80**, 890 (1998).
26. G. Roman-Perez, J. Soler, *Phys. Rev. Lett*. **103**, 096102 (2009).
27. A. Gulans, M.J. Puska, R.M. Nieminen, *Phys. Rev. B* **79**, 201105(R) (2009).
28. O.A. Vydrov, T. Van Voorhis, *Phys. Rev. Lett*. **103**, 063004 (2009).
29. J. Klimes, D.R. Bowler, A. Michaelides, *J. Phys. Condens. Matter* **22**, 022201 (2010).
30. E.R. Johnson, A.D. Becke, *J. Chem. Phys*. **123**, 024101 (2005).
31. P.L. Silvestrelli, *Phys. Rev. Lett*. **100**, 053002 (2008).
32. S. Grimme, J. Antony, S. Ehrlich, H. Krieg, *J. Chem. Phys*. **132**, 154104 (2010).
33. T. Thonhauser, V.R. Cooper, S. Li, A. Puzder, P. Hyldgaard, D.C. Langreth, *Phys. Rev. B* **76**, 125112 (2007).
34. N. Marom, A. Tkatchenko, M. Scheffler, L. Kronik, *J. Chem. Theory Comput*. **6**, 81 (2010).
35. W.G. Aulbur, L. Jönsson, J.W. Wilkins, *Solid State Phys.: Adv. Res. Appl*. **54**, 1 (2000).
36. F.S. Tautz, *Prog. Surf. Sci*. **82**, 479 (2007).
37. A. Hauschild, K. Karki, B.C.C. Cowie, M. Rohlfing, F.S. Tautz, M. Sokolowski, *Phys. Rev. Lett*. **94**, 036106 (2005).
38. Y. Zou, L. Kilian, A. Schöll, Th. Schmidt, R. Fink, E. Umbach, *Surf. Sci*. **600**, 1260 (2006).
39. P. Bagus, V. Staemmler, C. Wöll, *Phys. Rev. Lett* **89**, 096104 (2002).
40. U. Stahl, D. Gador, A. Soukopp, R. Fink, E. Umbach, *Surf. Sci*. **414**, 423 (1998).
41. J.B. Neaton, M.S. Hybertsen, S.G. Louie, *Phys. Rev. Lett*. **97**, 216405 (2006).
42. E. Zaremba, W. Kohn, *Phys. Rev. B* **13**, 2270 (1976).
43. N. Koch, *Chem. Phys. Chem*. **8**, 1438 (2007).
44. I.H. Campbell, J.D. Kress, R.L. Martin, D.L. Smith, N.N. Barashkov, J.P. Ferraris, *Appl. Phys. Lett*. **71**, 3528 (1997).
45. S. Kobayashi, T. Nishikawa, T. Takenobu, S. Mori, T. Shimoda, T. Mitani, H. Shimotani, N. Yoshimoto, S. Ogawa, Y. Iwasa, *Nat. Mater*. **3**, 317 (2004).
46. M. Pfeiffer, A. Beyer, T. Fritz, K. Leo, *Appl. Phys. Lett*. **73**, 3202 (1998).
47. W.Y. Gao, A. Kahn, *J. Appl. Phys*. **94**, 359 (2003).
48. N. Koch, S. Duhm, J.P. Rabe, A. Vollmer, R.L. Johnson, *Phys. Rev. Lett*. **95**, 237601 (2005).
49. H. Ishii, K. Sugiyama, E. Ito, K. Seki, *Adv. Mater*. **11**, 605 (1999).
50. S. Braun, W.R. Salaneck, M. Fahlman, *Adv. Mater*. **21**, 1450 (2009).
51. L. Romaner, G. Heimel, J.-L. Brédas, A. Gerlach, F. Schreiber, R.J. Johnson, J. Zegenhagen, S. Duhm, N. Koch, E. Zojer, *Phys. Rev. Lett*. **99**, 256801 (2007).
52. A.M. Track, F. Rissner, G. Heimel, L. Romaner, D. Käfer, A. Bashir, G.M. Rangger, O.T. Hofmann, T. Bucko, G. Witte, E. Zojer, *J. Phys. Chem. C*, **114**, 2677 (2010).
53. J. Harl, L. Schimka, G. Kresse, *Phys. Rev. B* **81**, 115126 (2010).
54. J. Perdew, K. Burke, M. Ernzerhof, *Phys. Rev. Lett*. **77**, 3865 (1996). □